Humidity-activated shape memory effect on plasticized starch-based biomaterials.

Valentina Sessini[a, b], Marina P. Arrieta[b], Alberto Fernández-Torres[b] and Laura Peponi[b*]

[a] *Dipartimento di Ingegneria Civile e Ambientale, Università di Perugia, Strada di Pentima, 05100 Terni, Italy*

[b] *Instituto de Ciencia y Tecnología de Polímeros, ICTP-CSIC, calle Juan de la Cierva 3, 28006, Madrid, Spain.*

ABSTRACT

Humidity-activated shape memory behaviour of plasticized starch-based films reinforced with the innovative combination of starch nanocrystals (SNCs) and catechin as antioxidant were studied. In a previous work, we reported the processing of gelatinized starch-based films filled with SNCs and catechin as antioxidant agent, and we observed that this novel combination leads to starch-based film with enhanced thermal and mechanical performance. In this work, the humidity-activated shape memory behavior of the previous developed starch-based films was characterized. The moisture loss as well as the moisture absorption were studied since they are essential parameters in humidity-activated shape memory polymers to fix the temporary shape and to recover the original shape, respectively. Therefore, the effect of the incorporation of SNCs and catechin on the humidity-activated shape memory properties of plasticized starch was also studied. Moreover, the effectiveness of catechin to increase the polymer stability under oxidative atmosphere and the thermo-mechanical relaxation of all the starch-based materials were studied. The combination of plasticized starch matrix loaded with both, SNCs and catechin, leads to a multifunctional starch-based films with increased hydrophilicity and with excellent humidity-activated shape memory behavior with interest for potential biomedical applications.

Highlights

- The humidity-activated shape memory behaviour of starch biomaterials was studied;
- The shape memory mechanism was based on the plasticizing effect of humidity;
- The presence of SNCs and Cat, produced a significant increase on the R_r values.

Keywords: starch, shape memory, bending, catechin, humidity.

1. Introduction

Shape memory polymers (SMPs) have gained considerable interest during the last years in both academics and industrial sector, focusing the attention on their potential application in the biomedical sector (Peponi, Navarro-Baena, & Kenny, 2014; Yahia, 2015). SMPs have the capacity to memorize their original shape after being deformed in a temporary shape under the application of external stimulus, such as temperature, humidity, pH, light, etc. (Olalla, Sessini, Torres, & Peponi, 2016). These shape changes are achieved throughout the "programming" and the "recovery" stages, regulated by the external stimulus (Peponi, Arrieta, Mujica-Garcia, & López, 2016). In the "programming" stage, the material is deformed and fixed in a "temporary shape". Then, upon the application of an external stimulus, the material recovers its initial shape throughout the "recovery" stage (Chan et al., 2016). One of the most used stimuli is the temperature, therefore, thermally-activated SMPs have to be heated above their characteristic transition temperature (T_{trans}) to induce their shape change (Peponi et al., 2017).

SMPs can be applied in several fields including biomedical applications. However, when SMPs are used for biomedical applications, two key points have to be considered. From one hand, the materials used need to respond to biocompatibility, non-toxicity,

biodegradability, sterilizability and specific mechanical properties (Ward Small, Singhal, Wilson, & Maitland, 2010). As example, biodegradable polymeric materials are being investigated in developing medical devices such as temporary biological wound dressing materials, temporary prostheses, three-dimensional porous structures as scaffolds for tissue engineering and for drug delivery in pharmacological applications (Arockianathan, Sekar, Kumaran, & Sastry, 2012; Nair & Laurencin, 2007). From the other hand, it is necessary to use a stimulus compatible with the human body (Chan et al., 2016; Lendlein, Behl, Hiebl, & Wischke, 2010). So, when working with thermally-activated SMPs for biomedical applications, a T_{trans} close to body temperature is required (Lendlein et al., 2010). In order to design SMPs with T_{trans} close to body temperature it is possible playing with their chemical composition or by adding nanofillers able to modify their thermal response (Behrens & Appel, 2016). However, moisture-activation of SMPs can be a good alternative as stimuli-responsive materials for biomedical applications (Chen, Hu, Yuen, & Chan, 2009; Sessini et al., 2016). Further investigations showed that the hydrogen bonding is the key player for the humidity activation as well as water absorbed in the polymer plays a main role in the shape recovery process (Zhang, Wang, Zhong, & Du, 2009). Therefore, in order to develop humidity-activated SMPs it is possible to use polymers with functional groups able to be involved in hydrogen bonding with water molecules or it is possible to use hydrophilic components.

Thus considering all these properties, biodegradability, hydrophilicity and biocompatibility, starch can be considered as an excellent material for the design of humidity-responsive SMPs for biomedical application. Starch, in fact, is a low cost polysaccharide, abundantly available in nature and one of the cheapest biodegradable polymers. It is produced by agricultural plants in the form of granules, which are hydrophilic (Raquez et al., 2008). Starch is mainly extracted from potatoes, corn, wheat,

rice, etc. It is composed of amylose (poly-α-1,4-D-glucopyranoside), a linear polymer and amylopectin (poly-α-1,4-D-glucopyranoside and α-1,6-D-glucopyranoside), a branched polymer (Lourdin et al., 2015). To extend the starch functionalities, several plants have been modified in their starch biosynthesis pathway to modulate the amount of amylose of starch granules (Firouzabadi, F. N., et al., 2007). In other cases starches are modified in their waxy form, for example characterized by a rich content of amylopectin (> 99%) to be used for the synthesis of starch nanocrystals, SNCs. (Bemiller, J. N., 1997). Therefore, starch can be used as polymer matrix in form of thermoplastic starch (TPS) by gelatinization of native starch (Averous, 2004) as well as nanofillers in form of starch nanocrystals, SNCs (Angellier, Choisnard, Molina-Boisseau, Ozil, & Dufresne, 2004). The glass transition temperature (T_g) of starch is strongly affected by the relative humidity (RH) at which it is stored showing either a glass-like rigid and fragile mechanical behavior, or a rubber-like behavior (Lourdin, Coignard, Bizot, & Colonna, 1997). However, the brittleness of starches is frequently overcome by the addition of plasticizers to get the flexibility required for film applications (Jiménez, Fabra, Talens, & Chiralt, 2012). Among them, glycerol is a natural plasticizer widely used to develop TPS by reducing intra and intermolecular hydrogen bonds (Arrieta, Peltzer, del Carmen Garrigós, & Jiménez, 2013; Averous, 2004; Jiménez et al., 2012). In the literature there are reports of different biomedical applications of biodegradable starch-based films as SMPs, such as shape-memory resorbable materials (Beilvert et al., 2014), temporary biological wound dressing materials (Arockianathan, Sekar, Kumaran, & Sastry, 2012), scaffolds for bone tissue engineering applications (Martins et al., 2012) and drug delivery systems (Schmitt et al., 2015). However, preliminary studies on shape memory effects on starch-based materials are presented by Chaunier et al. (Chaunier & Lourdin, 2009) in 2009 reporting an example of dual-shape capability of potato starch and by Véchambre et al. (Véchambre,

Chaunier & Lourdin, 2010) in 2010, in which they studied the shape memory response of extruded potato starch triggered by humidity.

In order to improve its properties starch can be modified by adding nanofillers obtaining nanocomposites. In general, the addition of nanofillers to a polymer matrix increases its mechanical strength and stiffness and sometimes can generate functional properties, originating from the synergetic effect between both components (Peponi, Puglia, Torre, Valentini, & Kenny, 2014). Among bionanofillers, special attention has been paid to SNCs (Lin, Huang, Chang, Anderson, & Yu, 2011).

Green tea polyphenols, in particularly catechin (Cat), have gain interest owing to their multiple biological effects due to their strong antioxidant capacity (Castro López et al., 2012). Catechin is also interesting from a processing point of view since their antioxidant activity protects the polymer matrices during thermal and thermomechanical processing (Arrieta et al., 2014). Moreover, catechin can be used to improve shape memory response of polymeric matrices (Arrieta, Sessini & Peponi, 2017).

In our previous work (Sessini, Arrieta, Kenny, & Peponi, 2016) we reported the processing of gelatinized starch-based films filled with SNCs and catechin as antioxidant agent for edible films. It was observed that for film manufacturing the inherent brittleness of starch can be overcome by the addition of 35 wt % of glycerol as plasticizer (S-Gly35). Additionally, we observed that the novel combination of plasticized starch compounded with both SNCs and Cat leads to materials with enhanced thermal and mechanical performance.

Based on these previous results, the main objective of the present work is to design high performance humidity-activated shape memory starch-based films, for potential biomedical applications. With this purpose, the humidity-activated shape memory behavior was characterized for neat starch plasticized with 35 % of glycerol and its filled counterparts. In order to know the parameters to fix the temporary shape and to

recover the original shape, the moisture loss as well as the moisture absorption was studied evaluating also the effect of the incorporation of both SNCs and catechin on the humidity-activated shape memory properties of plasticized starch-based films. Moreover, the effectiveness of catechin to increase the polymer stability under oxidative atmosphere and the thermo-mechanical relaxation of all the starch-based materials were studied in order to characterize their thermal properties.

2. Materials and Methods

2.1 Materials

Native potato starch (moisture content of 12 % and amylose content of 18 - 21 %) was kindly supplied by Novamont. Glycerol and catechin dehydrate were purchased from Panreac Quimica (PRS) and Sigma-Aldrich, respectively. Waxy maize starch (N200) used to synthesize the SNCs, was supplied by Roquette Laisa (Spain). Sulfuric acid (H_2SO_4) was purchased from Sigma-Aldrich. SNCs were synthesized by acid hydrolysis as reported in our previous work (Sessini et al., 2016). In brief, waxy maize starch was dispersed in an aqueous solution of H_2SO_4 and heated at 40 ºC under continuous mechanical stirring (100 rpm) for 5 days. The final suspensions were washed by successive centrifugations in distilled water (10,000 rpm for 10 minutes) until reaching neutral pH and then, it was filtered and stored at 4 ºC.

2.2 Film preparation

The starch-based films were obtained by gelatinization of starch/water/glycerol dispersion (Sessini et al., 2016). Briefly, TPS was successfully obtained by gelatinization of an aqueous dispersion of 1 wt % of potato starch and 35 wt % of glycerol relative to the mass of starch. The dispersion was gelatinized at 80 ºC during 15 min under continuous stirring. Starch solution, was cast over polystyrene petri dish in a

ventilated oven at 35 ºC for 24 h to obtain films with a thickness of about 100 µm. The obtained unfilled film was named S-Gly35. The polymeric matrix was reinforced by adding 1 wt % (relative to the mass of starch) of catechin (S-Gly35-Cat) and SNCs (S-Gly35-SNC), respectively. Moreover, the synergetic effect of both catechin and SNCs was evaluated in the starch-based films by adding together catechin and SNCs, both at 1 wt % relative to the mass of starch, obtaining the sample named S-Gly35-Cat-SNC.

2.3 Characterization Techniques

Before characterization, all the starch-based films were stored for one week at 50 % RH. The SNCs dispersion into the polymer matrix was studied by Field Emission Scanning Electron Microscope (FE-SEM, Hitachi S8000). The cryo-fracture surfaces of the starch-based films filled with SNCs were observed. The films were previously frozen using liquid N_2 and then cryo-fractured. All the samples were chrome coated by an automatic sputter coater Quorum Tech Q 150T ES previously to be observed by FE-SEM.

Differential Scanning Calorimetry (DSC) analysis was performed in a Mettler Toledo DSC822e instrument under oxygen atmosphere (30 mL/min). Samples were heated from 30 to 300 ºC at a heating rate of 10 ºC min^{-1} to determine the oxidation induction time (OIT) as well as the temperature at which a rapid increase in the rate of oxidation was observed (onset oxidation temperature, OOT). OIT and OOT values were calculated by extrapolating the tangent drawn on the steepest slope of exothermic reaction, which corresponds to the degradation, in the baseline (Erhan, Sharma, & Perez, 2006).

Dynamic Mechanical Thermal Analysis (DMTA) of the samples was carried out using a DMA Q800 from TA Instrument in film tension mode with an amplitude of 5 µm, a frequency of 1 Hz, a force track of 125 % and a heating rate of 2 ºC·min^{-1}. The samples

were cut from casted films into rectangular specimens of approximately 20 mm x 6 mm x 0.10 mm.

Surface wettability of the starch-based films was studied through static water contact angle (WCA) measurements using a KSV Theta goniometer. The volume of the droplets was controlled to be about 7.0 μL and a charge coupled device camera was used to capture the images of the water droplets for the determination of the contact angles. The contact angle was determined by randomly putting 4 drops of distilled water with a syringe onto the film surfaces and the average values were used.

Moisture absorption was tested at room temperature (RT) after specimens were dried in a dry chamber (RH ≤ 10 %). The samples were put on a humidity chamber at RH = 72 %. Saturated salt solutions were used to provide specific relative humidity. Weight percentage of specimen was weighted after each 5 min firstly, and then the moisturizing time increased gradually when its absorption speed was slow (Chen et al., 2009; Vogt, Soles, Lee, Lin, & Wu, 2005). Finally, the dependency of moisture absorption on time was obtained. The same method was used to test the dependency of moisture loss vs time. The specimens were put on a dry chamber (RH ≤ 10 %) at RT until reach the equilibrium.

Humidity-mechanical cyclical experiments were carried out by bending test. The programming stage was performed in a dry chamber (RH ≤ 10 %) at RT, then the recovery stage was achieved in a humidity chamber (RH = 72 %) at RT. The samples were cut from the casted films into rectangular specimens of approximately 40 mm x 15 mm x 0.10 mm.

The shape recovery ratio (R_r) was calculated from the ratio of the different angles before and after recovery using the recovered angles (Θ_r) and the deformed angles (Θ_d) in the temporary shape, as reported in the equation below:

$$R_r(\%) = \frac{(\theta_d - \theta_r)}{\theta_d} \times 100 \quad \text{Equation (1)}$$

The shape fixity ratio (R_f) can be calculated from the ratio of the fixed angle (Θ_f) and the Θ_d as shown in the follow equation:

$$R_f(\%) = \frac{\theta_f}{\theta_d} \times 100 \quad \text{Equation (2)}$$

The measure of the bending test angles has been carried out through an open source image-processing program, ImageJ. The measures have been taken for triplicate in order to calculate a standard deviation. Scheme 1 indicates the bending test procedure for studying the shape memory behaviour of the materials, indicating the recovered and deformed angles as well as the humidity corresponding to each phase of the programming and recovery analysis.

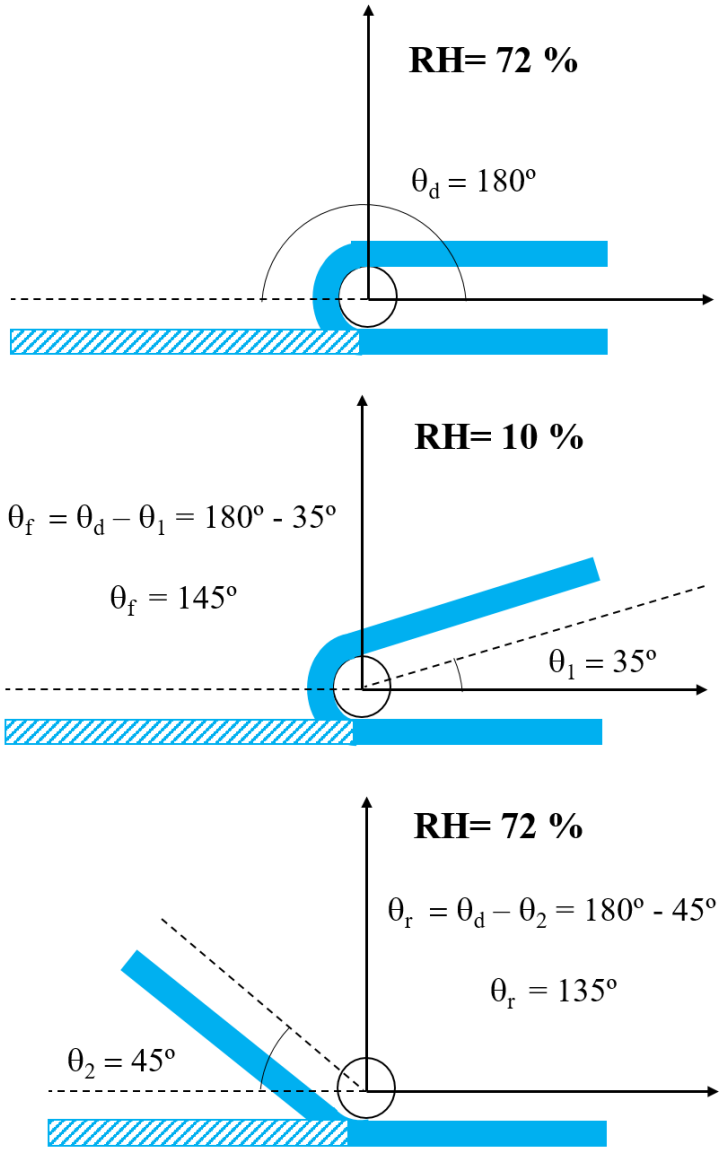

Scheme 1. Bending test procedure for studying the shape memory behaviour of the materials, indicating the recovered and deformed angles as well as humidity.

3. Results and Discussion

The cryo-fractured starch-based film surfaces (surface of rupture on the thickness of the film) were studied with FE-SEM in order to visualize the SNCs dispersion into the starch matrix. Figure 1 shows the cryo-fractured surface of the samples reinforced with SNCs, i.e. S-Gly35-SNC and S-Gly35-Cat-SNC. SNCs were visible in the FE-SEM

images, confirming their good dispersion into the plasticized starch-based film (See arrows in Figure 1).

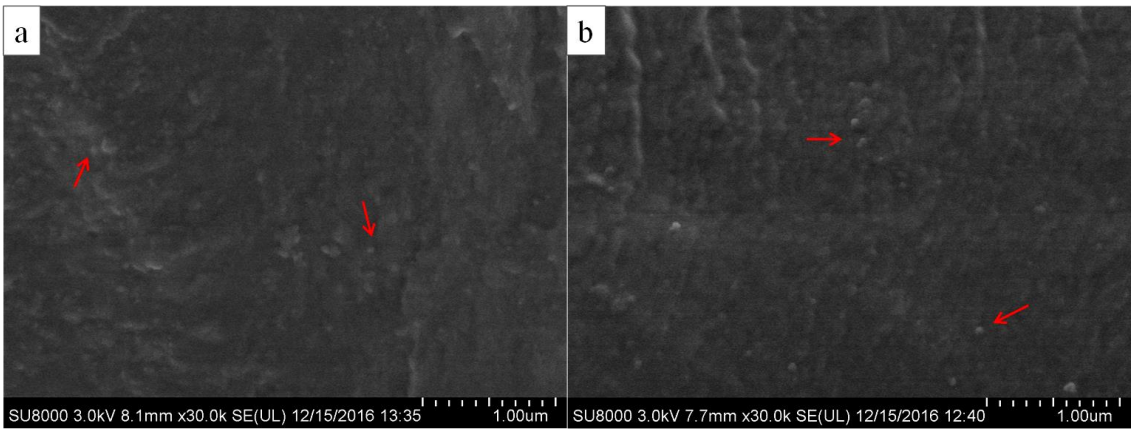

Figure 1. FE-SEM images of the cryo-fractured surface of the starch-based materials reinforced with SNCs; a) S-Gly35-SNC and b) S-Gly35-Cat-SNC.

In order to study the main thermo-mechanical relaxation of our systems, DMTA was performed. The evolution of the storage modulus (E'), loss modulus (E'') and damping factor (tan δ) as a function of temperature was measured over the temperature range of -80 ºC to 100 ºC and the results are presented in Figure 2. At temperature -80 ºC, all the starch-based films exhibit high storage modulus values, indicating the rigidity of the freeze structure below T_g. The storage modulus falls in two steps, the first between -80 and -30 ºC and the second one, less evident, between -30 and 40 ºC with the corresponding peaks in the loss modulus curve (Figure 2.b) around -47 ºC and 21 ºC, respectively. It was previously reported in the literature that for starch-based materials constituted by the three-constituent system such as water-glycerol-starch, the roles of the two plasticizers (glycerol and water) are dependent on their respective concentration (Lourdin, Bizot, & Colonna, 1997). In fact, depending on the plasticizer content, starch can show two different structural relaxations corresponding to a non-homogeneous material constituted by two different phases, a glycerol-rich phase and a starch-rich phase (Liu, Bhandari, & Zhou, 2006).

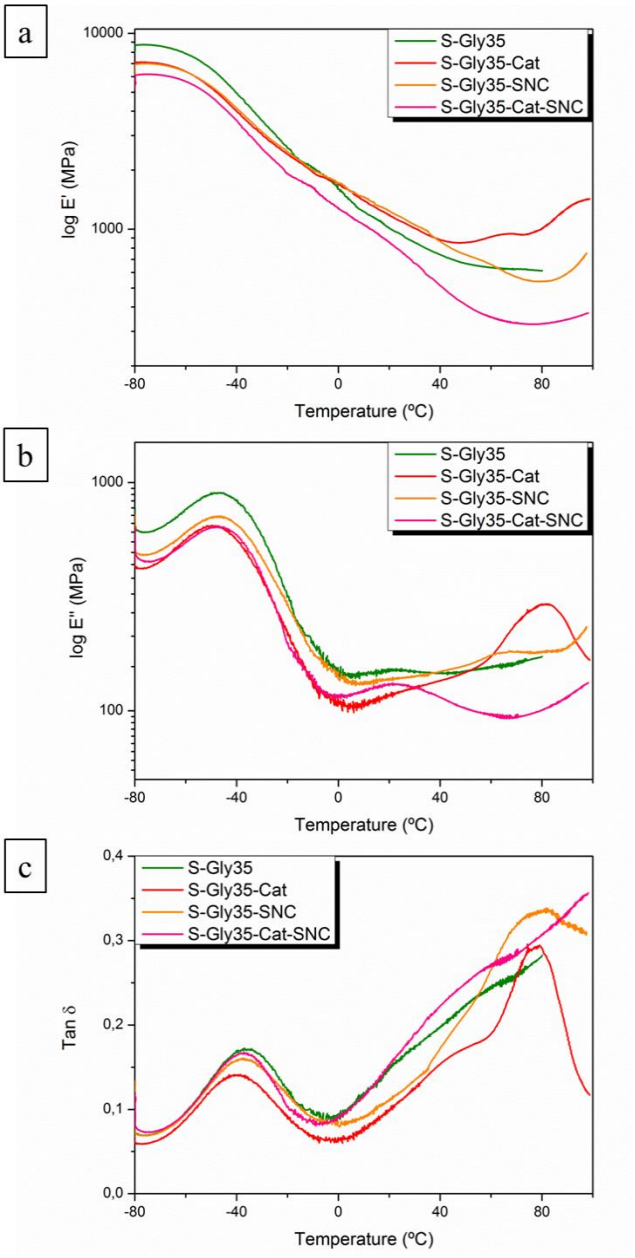

Figure 2. Dynamic mechanical thermal analysis, a) storage modulus, b) loss modulus and c) damping factor, for all the starch-based films.

In our case, the results observed in Figure 2.b suggest that by using 35 wt % of glycerol, two glass transitions of a phase-separated system on all the starch-based film curves can be observed. The first peak in the loss modulus curves (Figure 2.b), named β relaxation, is due to the glycerol-rich phase. The second peak in the loss modulus curve (Figure 2.b) around 21 ºC, named α relaxation, was attributed to the T_g of starch, confirming previous results reported in literature (Forssell, Mikkilä, Moates, & Parker, 1997). As it

is shown in Figure 2.b and c, it can be concluded that the fillers does not disturb the mobility of glycerol-rich phase. On the contrary, when the SNCs were added into the starch-based matrix, the α relaxation is found to increase and to shift to higher values of temperature, even more when only Cat were added. This is an indication that the presence of the filler hinders the molecular mobility of amylopectin chains, in agreement with the results obtained also by Viguié et al. (Viguié, Molina-Boisseau, & Dufresne, 2007) for plasticized waxy maize starch reinforced with SNCs. Viguié et al. reported that this phenomenon is most probably ascribed to a direct contact between amylopectin-rich domains of the matrix and starch nanocrystals, and to the formation of strong interactions between both components due to hydrogen bonding (Viguié et al., 2007). Thus, in our case, SNCs and particularly Cat (S-Gly35-SNC and S-Gly35-Cat), hindered the molecular mobility of amylopectin chains probably due to the formation of hydrogen bonding. In the case of S-Gly35-Cat-SNC, where 1 % of both, Cat and SNCs, were added into the starch-based films, α relaxation temperature evidently decreased compare to the other filled films.

The temperatures of relaxation observed are summarized on Table 1.

Table 1: Summary of the relaxation temperatures taken from loss modulus diagram.

Sample	β-relaxation (°C)	α-relaxation (°C)
S-Gly35	-45	21
S-Gly35-Cat	-49	79
S-Gly35-SNC	-46	64
S-Gly35-Cat-SNC	-45	25

This result suggests that the presence of SNCs probably weakness the interchain interactions between starch matrix and catechin leading to an increase of molecular mobility of amylopectin chains and thus recovering the same mobility of its neat counterpart.

Starch-based materials are highly sensitive to humidity and their T_g decrease upon the water content absorbed into the material. Indeed, the humidity is capable to depress the glass transition of starch below room temperature. Lourdin et al. (Lourdin et al., 1997) reported that the T_g of potato starch occurs below or above room temperature as a function of both the plasticizer and the water content. They showed that for potato starch with 35 wt % of glycerol, a content of water higher than 13 wt % is necessary to obtain a T_g below room temperature. Therefore, humidity is used as external stimulus needed by these starch-based materials to present humidity-activated shape memory behavior at room temperature due to the plastificant effect of water. At RH = 72 % the materials present a rubber-like behaviour, thus it was possible to modify their shape and to fix the temporary shape only reducing the RH. In fact at RH = 10 % the materials present a glass-like rigid behavior and they were capable to fix their temporary shape. Finally the recovery was activated with humidity (RH = 72 %). The materials became rubber-like again and the forces stored into the material during the programming, drove the recovery process. For that reason, the shape memory mechanism proposed here depends on the plasticizing effect of humidity on starchy materials.

Therefore, in order to define how many minutes are needed to activate both programming and recovery steps in the humidity-mechanical cycles used for the evaluation of the humidity-activated shape memory behavior, the dependency of moisture loss as well as of its absorption as a function of time were studied at RT. Figure 3.a and b present the dependencies of the moisture loss (fundamental for the temporary shape fixity) and the moisture absorption (fundamental for the original shape

recovery) with time for all the starch-based films. In Figure 3.a, it can be observed that all the starch-based films lost the moisture very quickly within the first 90 min, showing the same slope of the moisture loss curves for all the samples analyzed. Then, they tend to reach their equilibrium state after 300 min. Whereas, in S-Gly35-SNC the wt % of moisture lost was pretty much the same of its neat counterpart (S-Gly35). In the case of S-Gly35-Cat the wt % of moisture lost is lower than S-Gly35, and even more for S-Gly35-Cat-SNC. The same trend is shown in Figure 3.b for the moisture absorption. Indeed S-Gly35 and S-Gly35-SNC followed the same trend of moisture absorption, absorbing around 19 wt % of water at the equilibrium, 16 wt % for S-Gly35-Cat and 13 wt % for S-Gly35-Cat-SNC have been obtained. The results showed that the presence of catechin in the starch matrix decreased the total wt % of moisture lost and absorbed, decreasing evens more with the presence of SNCs. Considering the high amount of hydroxyl groups on catechin and SNCs surfaces, it is expected that they will interact with water since the amount of water uptake is directly related with their polar free fraction able to interact with water (Arrieta et al., 2014).

Nevertheless, in the case of S-Gly35-Cat-SNC, the well interaction established between catechin and SNCs, leaded to less available -OH groups of both materials to interact with water, and thus S-Gly35-Cat-SNC formulation shows the lowest water absorption.

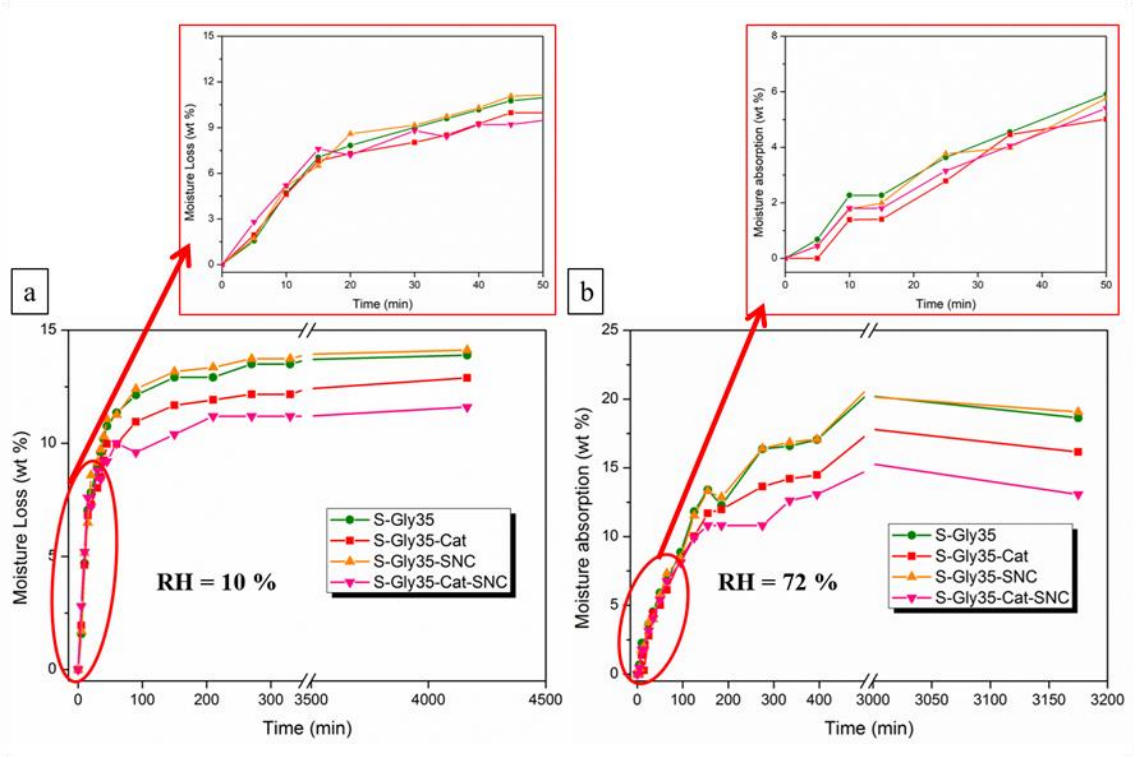

Figure 3. Dependencies on time of: a) moisture loss and b) moisture absorption.

The less water absorption was followed by the S-Gly35-Cat starch-based film since their -OH groups can interact better with plasticized starch matrix than SNCs, as it was already commented in DMTA results. For all starch-based films the slop of moisture loss (Figure 3.a) was much higher than that of moisture absorption (Figure 3.b) showing a faster kinetic for moisture loss process. In fact, in Figure 3.b, it can be observed that all the starch-based films absorbed much moisture within the first 150 min and then they tend to reach their saturated state after 450 minutes though they reach a middle maximum due to the swelling-deswelling phenomenon known as "overshooting effect" (Yin, Ji, Dong, Ying, & Zheng, 2008; Zhu, Ma, Wang, Zhang, & Zhang, 2016), then they reached the equilibrium.

However, in order to study the shape memory behaviour it is not necessary that the samples reach their equilibrium state. And from the zoom of both graphics of the moisture loss and moisture absorption, it is possible to see that their activation starts at

about 20 minutes. For this reason a time of 40 minutes has been choose for studying the shape memory response of these starch-based materials.

Therefore, we determined the conditions to be used for the humidity-mechanical cycles performed in the bending test configuration at RT:

- Programming: conditioning the sample at RH = 72 % for 40 minutes and then bending the samples under humidity conditions. Drying the samples at RH ≤ 10 % for 40 minutes under constant bending.
- Recovery: releasing the bending in dry condition to obtain the fixation of temporary shape and recovering the original shape at RH = 72 % for 40 minutes.

These experimental conditions confirm that a time of 40 min is enough to change the physical behaviour of the starch-based material. In order to evaluate their shape-memory response, four different humidity-mechanical cycles were completed for each sample. In Figure 4, an example of humidity-mechanical bending cycle for all the materials is reported.

The R_r and R_f values obtained for each cycle of the starch-based films are reported in Table 2. The presence of both fillers, SNCs and Cat, produced a significant increase on the shape recovery ratio showing that the presence of particles gives higher stiffness to the systems allowing the better recovery of their original shape.

Table 2. R_r and R_f values for all the humidity-activated bending cycles performed for all the samples studied.

Sample	**R_r (%)**				**R_f (%)**			
Cycle	*1*	*2*	*3*	*4*	*1*	*2*	*3*	*4*
S-Gly35	95±2	91±1	89±1	89±1	96±1	99±1	98±1	94±1
S-Gly35-Cat	98±1	99±1	99±1	99±1	97±1	96±1	96±2	98±1

S-Gly35-SNC	99±1	98±1	99±1	98±1	98±1	97±1	98±1	97±1
S-Gly35-Cat-SNC	95±1	97±1	96±1	98±1	98±1	96±1	96±1	93±1

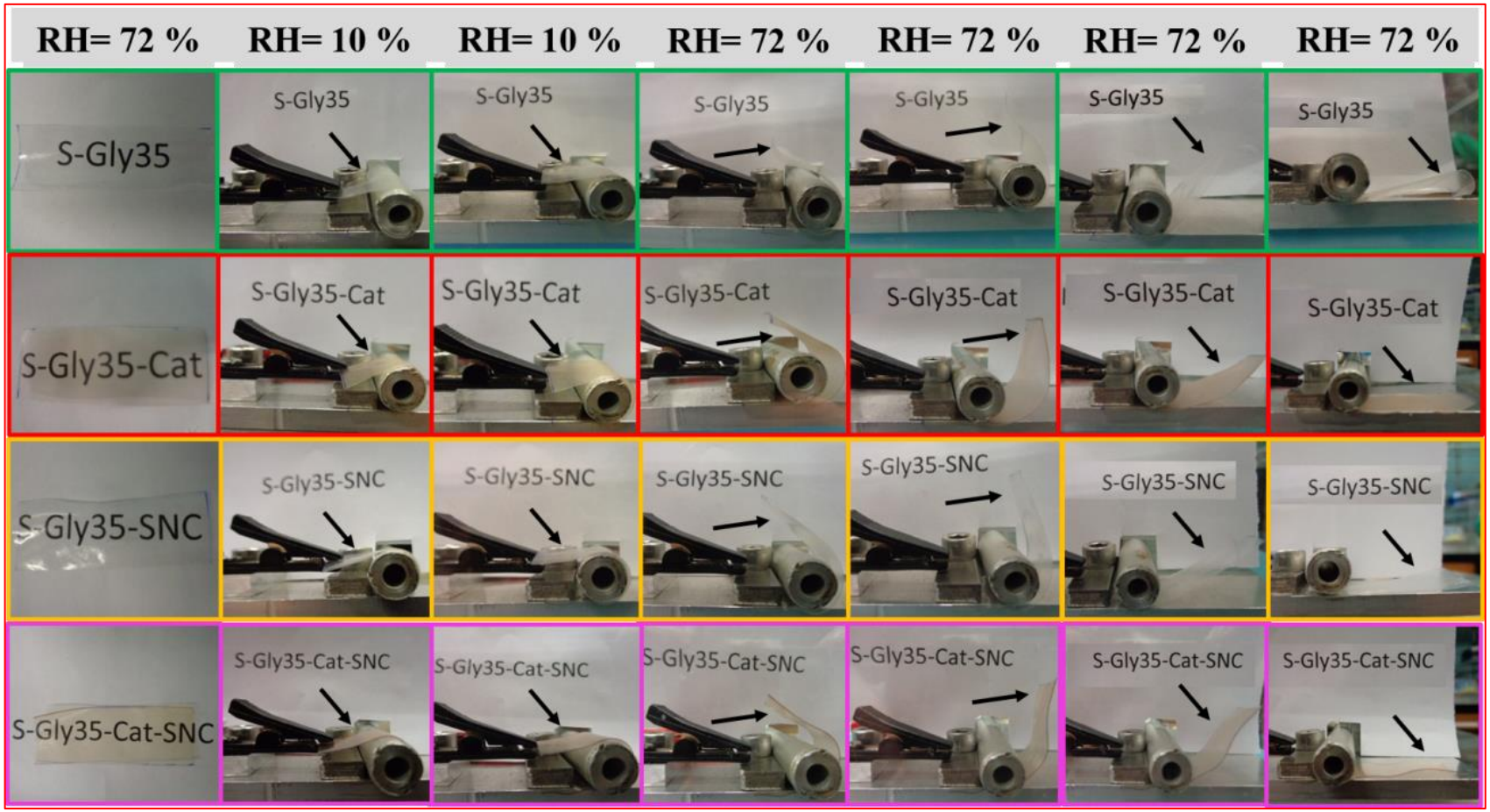

Figure 4. Example of humidity-activated bending cycles for all the starch-based films.

In Table 2 it is easy to note that the obtained R_f and R_r values reflect the excellent ability to both, fix the temporary and recover the original shape, respectively, even for the neat starch-based film, S-Gly35. The R_r values increased for S-Gly35-Cat, S-Gly35-SNC and S-Gly35-Cat-SNC, reaching values close to 100 %, increasing the recovery ability of the neat matrix. Moreover, R_f, close to 100 % for the neat matrix, did not change with the addition of the fillers to the matrix.

In order to study the possible biomedical application of these shape memory starch-based materials, the wettability and hydrophobic characteristics of their surfaces were determined from WCA measurements. It is known that the WCA is dependent on the cohesive and adhesive molecular forces within water and between the solid surface and water, respectively. A WCA higher than 65º is typical used as a threshold for hydrophobic surfaces, meanwhile WCA lower than 65º are related to hydrophilic surfaces (Arrieta et al., 2014; Vogler, 1998).

Surface wettability of artificial materials for biomedical applications is one of the most important factors affecting the cells adhesion. In fact, cells adhesion is not good on surfaces having too low or too high wettability (Wang et al., 2012; Yuan et al., 2013). In particular, with respect to surface wettability of polymeric materials, cells effectively adhere onto polymer surfaces presenting moderate wettability that is with WCA in the range of 40-70º (Arima & Iwata, 2007). In Figure 5, the WCA values for all the starch-based materials are reported. S-Gly35 showed a WCA of 83±4º, while the other films showed lower WCA. This means that the incorporation of SNCs and catechin increases the wettability of the starch-based films. Indeed when SNCs were added to the system, the contact angle decrease until 66±3º and when catechin was added a contact angle of 63±3º was reported.

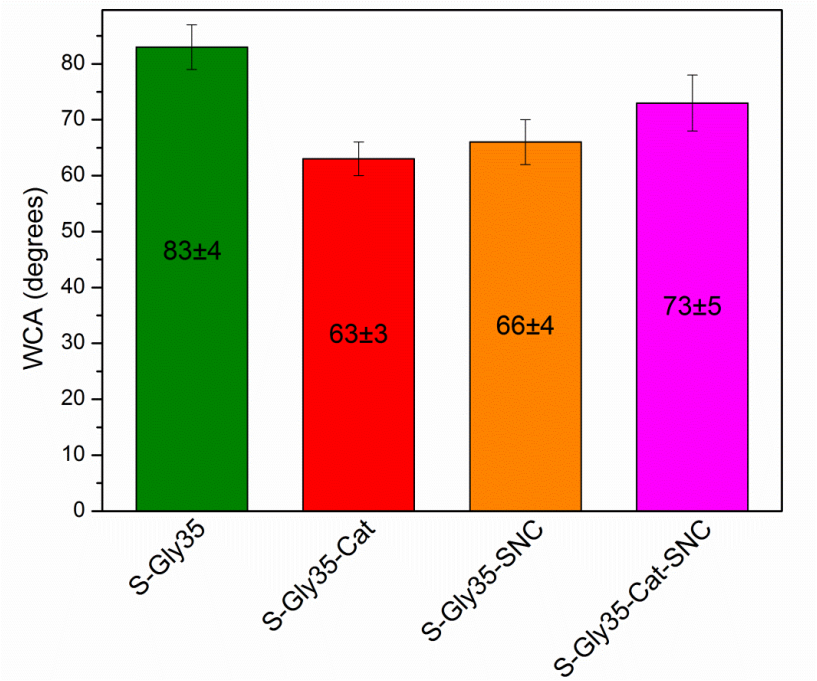

Figure 5. Wettability of all the starch-based films.

The decrease in WCA of the filled films is related with the high amount of –OH groups of catechin and SNCs whit surface orientation, which interact with the water at the material surfaces leading to more hydrophilic surfaces (M. Arrieta, López, López, Kenny, & Peponi, 2016). On the contrary, when both particles were incorporated to the starch matrix, the WCA increased compared to the other filled films, but it still decreases compared to its neat counterpart. The higher WCA observed in S-Gly35-Cat-SNC with respect to the other filled films could be related with the fact that some –OH groups of catechin and SNCs are interacting between them and thus are less available to interact with the water molecules at the material surfaces, thus confirming our previous results. However, it can be concluded that the obtained starch-based films, present the ideal moderate wettability needed for cells adhesion and that they might be use as potential shape-memory materials for biomedical applications.

4. Conclusions

In this work, the humidity-activated shape memory behaviour of starch-based film reinforced with the innovative combination of SNCs and the antioxidant catechin were studied. FE-SEM showed well dispersed SNCs while DSC analysis under oxidative conditions revealed that catechin protect the starch-based matrix against thermo-oxidation. The addition of both particles to the polymeric matrix produced materials with more hydrophilic surfaces due to the surface orientation of -OH groups. Meanwhile, the positive interaction between Cat and SNCs into the S-Gly35-Cat-SNC starch-based film leads to a material with reduced moisture loss as well as reduced moisture absorption. The influence of catechin and SNCs addition on their thermal relaxation was studied by DMA and it showed that the combination of both particles probably weakness the interchain interactions between starch and catechin leading to an increase of molecular mobility of amylopectin chains. The plasticizing effect of moisture on starchy materials was the mechanism involved in the humidity-activated shape memory behavior, depressing the glass transition of starch below room temperature. Therefore, actuation of this starch-based material can be achieved at room temperature only using humidity. The obtained R_f and R_r values reflect the excellent ability to both, fix and recover the temporary and original shape respectively, even for the neat film. The presence of both fillers, SNCs and Cat, produced a significant increase on the shape recovery ratio values allowing a better recuperation of the original shape.

The combination of plasticized starch matrix loaded with both, SNCs and Cat particles, leads to a multifunctional starch-based film with increased hydrophilicity and with humidity-activated shape memory behavior with interest for potential biomedical applications.

Acknowledgements

Authors thank Spanish Ministry of Economy and Competitiveness, MINECO, (MAT2013-48059-C2-1-R). M.P.A. and L.P. acknowledge the Juan de la Cierva (FJCI-2014-20630) and Ramon y Cajal (RYC-2014-15595) contracts from the MINECO, respectively. Authors thanks also CSIC for the I-LINK project, I-LINK1149.

References

Angellier, H., Choisnard, L., Molina-Boisseau, S., Ozil, P., & Dufresne, A. (2004). Optimization of the preparation of aqueous suspensions of waxy maize starch nanocrystals using a response surface methodology. *Biomacromolecules*, 5(4), 1545-1551.

Arima, Y., & Iwata, H. (2007). Effect of wettability and surface functional groups on protein adsorption and cell adhesion using well-defined mixed self-assembled monolayers. *Biomaterials*, 28(20), 3074-3082.

Arockianathan, P. M., Sekar, S., Kumaran, B., & Sastry, T. (2012). Preparation, characterization and evaluation of biocomposite films containing chitosan and sago starch impregnated with silver nanoparticles. *International journal of biological macromolecules*, 50(4), 939-946.

Arrieta, M., López, J., López, D., Kenny, J., & Peponi, L. (2016). Effect of chitosan and catechin addition on the structural, thermal, mechanical and disintegration properties of plasticized electrospun PLA-PHB biocomposites. *Polymer Degradation and Stability*, 132, 145-156.

Arrieta, M. P., Castro-López, M. a. d. M., Rayón, E., Barral-Losada, L. F., López-Vilariño, J. M., López, J., & González-Rodríguez, M. V. (2014). Plasticized poly (lactic acid)–poly (hydroxybutyrate)(PLA–PHB) blends incorporated with catechin intended for active food-packaging applications. *Journal of agricultural and food chemistry*, 62(41), 10170-10180.

Arrieta, M. P., Peltzer, M. A., del Carmen Garrigós, M., & Jiménez, A. (2013). Structure and mechanical properties of sodium and calcium caseinate edible active films with carvacrol. *Journal of Food Engineering*, 114(4), 486-494.

Arrieta, M. P., Peltzer, M. A., López, J., del Carmen Garrigós, M., Valente, A. J., & Jiménez, A. (2014). Functional properties of sodium and calcium caseinate antimicrobial active films containing carvacrol. *Journal of Food Engineering*, 121, 94-101.

Arrieta, M. P., Sessini, V. & Peponi, L. (2017). Biodegradable poly(ester-urethane) incorporated with catechin with shape memory and antioxidant activity for food packaging. *European Polymer Journal*, 94, 111-124.

Averous, L. (2004). Biodegradable multiphase systems based on plasticized starch: a review. *Journal of Macromolecular Science, Part C: Polymer Reviews*, 44(3), 231-274.

Behrens, S., & Appel, I. (2016). Magnetic nanocomposites. *Current opinion in biotechnology*, 39, 89-96.

Beilvert, A., Chaubet, F., Chaunier, L., Guilois, S., Pavon-Djavid, G., Letourneur, D., . . . Lourdin, D. (2014). Shape-memory starch for resorbable biomedical devices. *Carbohydrate Polymers*, 99, 242-248.

Bemiller, J. N. (1997). Starch modification: challenges and prospects. *Starch-Stärke*, *49*(4), 127-131.

Castro López, M. d. M., Pérez, M. C., García, M. S. D., Vilarino, J. M. L., Rodríguez, M. V. G., & Losada, L. F. B. (2012). Preparation, evaluation and characterization of quercetin-molecularly imprinted polymer for preconcentration and clean-up of catechins. *Analytica chimica acta*, 721, 68-78.

Chan, B. Q. Y., Low, Z. W. K., Heng, S. J. W., Chan, S. Y., Owh, C., & Loh, X. J. (2016). Recent advances in shape memory soft materials for biomedical applications. *ACS applied materials & interfaces*, 8(16), 10070-10087.

Chaunier, L., & Lourdin, D. (2009). The shape memory of starch. *Starch/Stärke*, 61 (2), 116-118.

Chen, S., Hu, J., Yuen, C.-w., & Chan, L. (2009). Novel moisture-sensitive shape memory polyurethanes containing pyridine moieties. *Polymer*, 50(19), 4424-4428.

Erhan, S. Z., Sharma, B. K., & Perez, J. M. (2006). Oxidation and low temperature stability of vegetable oil-based lubricants. *Industrial Crops and Products*, 24(3), 292-299.

Firouzabadi, F. N., Vincken, J. P., Ji, Q., Suurs, L. C., Buléon, A., & Visser, R. G. (2007). Accumulation of multiple-repeat starch-binding domains (SBD2–SBD5) does not reduce amylose content of potato starch granules. *Planta*, 225(4), 919-933.

Forssell, P. M., Mikkilä, J. M., Moates, G. K., & Parker, R. (1997). Phase and glass transition behaviour of concentrated barley starch-glycerol-water mixtures, a model for thermoplastic starch. *Carbohydrate Polymers*, 34(4), 275-282.

Jiménez, A., Fabra, M. J., Talens, P., & Chiralt, A. (2012). Edible and biodegradable starch films: a review. *Food and Bioprocess Technology*, 5(6), 2058-2076.

Lendlein, A., Behl, M., Hiebl, B., & Wischke, C. (2010). Shape-memory polymers as a technology platform for biomedical applications. *Expert Review of Medical Devices*, 7(3), 357-379.

Lin, N., Huang, J., Chang, P. R., Anderson, D. P., & Yu, J. (2011). Preparation, modification, and application of starch nanocrystals in nanomaterials: a review. *J. Nanomaterials*, 2011, 1-13.

Liu, Y., Bhandari, B., & Zhou, W. (2006). Glass transition and enthalpy relaxation of amorphous food saccharides: a review. *Journal of agricultural and food chemistry*, 54(16), 5701-5717.

Lourdin, D., Bizot, H., & Colonna, P. (1997). "Antiplasticization" in starch+glycerol films? *Journal of Applied Polymer Science*, 63(8), 1047-1053.

Lourdin, D., Coignard, L., Bizot, H., & Colonna, P. (1997). Influence of equilibrium relative humidity and plasticizer concentration on the water content and glass transition of starch materials. *Polymer*, 38(21), 5401-5406.

Lourdin, D., Putaux, J.-L., Potocki-Véronèse, G., Chevigny, C., Rolland-Sabaté, A., & Buléon, A. (2015). *Crystalline structure in starch*. In *Starch* (pp. 61-90): Springer

Marie Arockianathan, P., Sekar, S., Kumaran, B., & Sastry, T. P. (2012). Preparation, characterization and evaluation of biocomposite films containing chitosan and sago starch impregnated with silver nanoparticles. *International journal of biological macromolecules*, 50(4), 939-946.

Martins, A. M., Kretlow, J. D., Costa-Pinto, A. R., Malafaya, P. B., Fernandes, E. M., Neves, N. M., . . . Reis, R. L. (2012). Gradual pore formation in natural origin scaffolds throughout subcutaneous implantation. *Journal of Biomedical Materials Research Part A*, 100A(3), 599-612.

Nair, L. S., & Laurencin, C. T. (2007). Biodegradable polymers as biomaterials. *Progress in Polymer Science*, 32(8–9), 762-798.

Olalla, A. S., Sessini, V., Torres, E. G., & Peponi, L. (2016), 9 - *Smart Nanocellulose Composites With Shape-Memory Behavior*. In D. Puglia, E. Fortunati, & J. M. Kenny (Eds.), *Multifunctional Polymeric Nanocomposites Based on Cellulosic Reinforcements* (pp. 277-312), William Andrew Publishing

Peponi, L., Arrieta, M. P., Mujica-Garcia, A., & López, D. (2016), 6 - *Smart Polymers.* In C. F. Jasso-Gastinel,.& J. M. Kenny (Eds.), *Modification of Polymer Properties* (pp. 131-154), William Andrew Publishing

Peponi, L., Navarro-Baena, I., & Kenny, J. M. (2014), 7 - *Shape memory polymers: Properties, synthesis and applications*. In M. R. Aguilar De Armas, & J. S. Román (Eds.), *Smart Polymers and their Applications* (pp. 204-236), Woodhead Publishing

Peponi, L., Puglia, D., Torre, L., Valentini, L., & Kenny, J. M. (2014). Processing of nanostructured polymers and advanced polymeric based nanocomposites. *Materials Science and Engineering R: Reports*, 85(1), 1-46.

Raquez, J.-M., Nabar, Y., Srinivasan, M., Shin, B.-Y., Narayan, R., & Dubois, P. (2008). Maleated thermoplastic starch by reactive extrusion. *Carbohydrate Polymers*, 74(2), 159-169.

Schmitt, H., Creton, N., Prashantha, K., Soulestin, J., Lacrampe, M. F., & Krawczak, P. (2015). Melt-blended halloysite nanotubes/wheat starch nanocomposites as drug delivery system. *Polymer Engineering & Science*, 55(3), 573-580.

Sessini, V., Arrieta, M. P., Kenny, J. M., & Peponi, L. (2016). Processing of edible films based on nanoreinforced gelatinized starch. *Polymer Degradation and Stability*, 132, 157-168.

Sessini, V., Raquez, J.-M., Lo Re, G., Mincheva, R., Kenny, J. M., Dubois, P., & Peponi, L. (2016). Multiresponsive Shape Memory Blends and Nanocomposites Based on Starch. *ACS applied materials & interfaces,* 8(30), 19197-19201.

Véchambre, C., Chaunier, L., & Lourdin, D. (2010). Novel shape-memory materials based on potato starch. *Macromolecular Materials and Engineering*, 295(2), 115-122.

Viguié, J., Molina-Boisseau, S., & Dufresne, A. (2007). Processing and characterization of waxy maize starch films plasticized by sorbitol and reinforced with starch nanocrystals. *Macromolecular bioscience,* 7(11), 1206-1216.

Vogler, E. A. (1998). Structure and reactivity of water at biomaterial surfaces. *Advances in colloid and interface science,* 74(1), 69-117.

Vogt, B. D., Soles, C. L., Lee, H.-J., Lin, E. K., & Wu, W.-l. (2005). Moisture absorption into ultrathin hydrophilic polymer films on different substrate surfaces. *Polymer,* 46(5), 1635-1642.

Wang, H., Feng, Y., An, B., Zhang, W., Sun, M., Fang, Z., Khan, M. (2012). Fabrication of PU/PEGMA crosslinked hybrid scaffolds by in situ UV photopolymerization favoring human endothelial cells growth for vascular tissue engineering. *Journal of Materials Science: Materials in Medicine,* 23(6), 1499-1510.

Ward Small, I., Singhal, P., Wilson, T. S., & Maitland, D. J. (2010). Biomedical applications of thermally activated shape memory polymers. *Journal of materials chemistry,* 20(17), 3356-3366.

Yahia, L. (2015). *Shape memory polymers for biomedical applications*: Elsevier.

Yin, Y., Ji, X., Dong, H., Ying, Y., & Zheng, H. (2008). Study of the swelling dynamics with overshooting effect of hydrogels based on sodium alginate-g-acrylic acid. *Carbohydrate Polymers*, 71(4), 682-689.

Yuan, W., Feng, Y., Wang, H., Yang, D., An, B., Zhang, W., . . . Guo, J. (2013). Hemocompatible surface of electrospun nanofibrous scaffolds by ATRP modification. *Materials Science and Engineering: C*, 33(7), 3644-3651.

Zhang, H., Wang, H., Zhong, W., & Du, Q. (2009). A novel type of shape memory polymer blend and the shape memory mechanism. *Polymer*, 50(6), 1596-1601.

Zhu, B., Ma, D., Wang, J., Zhang, J., & Zhang, S. (2016). Multi-responsive hydrogel based on lotus root starch. *International journal of biological macromolecules*, 89, 599-604.